Isolated Mitochondria Transfer Improves Neuronal Differentiation of Schizophrenia-Derived Induced Pluripotent Stem Cells and Rescues Deficits in a Rat Model of the Disorder

Odile Robicsek[1,5], **Hila M. Ene**[1,5], **Rachel Karry**[1], **Ofer Ytzhaki**[1], **Eyal Asor**[1], **Donna McPhie**[2], **Bruce M. Cohen**[2], **Rotem Ben-Yehuda**[3], **Ina Weiner**[3,4], and **Dorit Ben-Shachar**[*,1]

[1]Laboratory of Psychobiology, Department of Psychiatry, Rambam Health Care Campus, B. Rappaport Faculty of Medicine and Rappaport Family Institute for Research in Medical Sciences, Technion IIT, Haifa, Israel; [2]Department of Psychiatry, Harvard Medical School, Boston, McLean Hospital, Belmont, MA; [3]School of Psychological Sciences, Tel Aviv University, Tel Aviv, Israel; [4]Sagol School of Neuroscience, Tel Aviv University, Tel Aviv, Israel

[5]These authors contributed equally to the article.

*To whom correspondence should be addressed; Laboratory of Psychobiology, Department of Psychiatry, Rambam Health Care Campus and B. Rappaport Faculty of Medicine, Technion ITT, POB 9649, Haifa 31096, Israel; tel: +972-4-8295224, fax: +972-4-8295220, e-mail: shachar@technion.ac.il

Dysfunction of mitochondria, key players in various essential cell processes, has been repeatedly reported in schizophrenia (SZ). Recently, several studies have reported functional recovery and cellular viability following mitochondrial transplantation, mostly in ischemia experimental models. Here, we aimed to demonstrate beneficial effects of isolated active normal mitochondria (IAN-MIT) transfer in vitro and in vivo, using SZ-derived induced pluripotent stem cells (iPSCs) differentiating into glutamatergic neuron, as well as a rodent model of SZ. First, we show that IAN-MIT enter various cell types without manipulation. Next, we show that IAN-MIT transfer into SZ-derived lymphoblasts induces long-lasting improvement in various mitochondrial functions including cellular oxygen consumption and mitochondrial membrane potential ($\Delta\psi_m$). We also demonstrate improved differentiation of SZ-derived iPSCs into neurons, by increased expression of neuronal and glutamatergic markers β3-tubulin, synapsin1, and Tbr1 and by an activation of the glutamate-glutamine cycle. In the animal model, we show that intra-prefrontal cortex injection of IAN-MIT in adolescent rats exposed prenatally to a viral mimic prevents mitochondrial $\Delta\psi_m$ and attentional deficit at adulthood. Our results provide evidence for a direct link between mitochondrial function and SZ-related deficits both in vitro and in vivo and suggest a therapeutic potential for IAN-MIT transfer in diseases with bioenergetic and neurodevelopmental abnormalities such as SZ.

Key words: isolated active normal mitochondria transfer/mitochondrial function/hiPSCs-derived neurons/prenatal poly-I:C rat model/attentional deficit/schizophrenia

Introduction

Mitochondria are responsible for many key cellular processes, including energy production, intracellular calcium buffering, apoptosis, and reactive oxygen species (ROS) production, all essential for cell development, function, and survival. In brain, with its high-energy requirements, mitochondrial deficits were shown to be associated with various anomalies, including in neuronal development, axonal growth, synaptic morphogenesis, and plasticity.[1–7] Accordingly, impairments in mitochondria are consistently observed in neurological and psychiatric disorders.[7–9] In schizophrenia (SZ), multifaceted mitochondrial dysfunctions were described including genetic modifications, alterations in mitochondrial transcriptome and proteome, functional aberrations in cellular respiration and in the oxidative phosphorylation system (OXPHOS), dissipation of $\Delta\psi_m$, and abnormal mitochondrial network dynamics.[10–15]

Several studies suggest that mitochondria can transfer between cells through various contact modes, including junction, cell fusion, and tunneling nanotube formation, contributing to the rescue of injured cells.[16–18] Transfer of mitochondria between cells has been shown to improve aerobic respiration in mammalian cell cultures and

protect from ischemia-reperfusion injury in animal models.[19,20] Recently, it was reported that functional mitochondria released by astrocytes can enter neurons in mice and enhance cell survival signals after cerebral ischemia. In addition, transfer of isolated mitochondria enhanced myocardial post-ischemic functional recovery in animal models of myocardial ischemia and reperfusion.[21,22]

Here, we show in vitro that isolated active normal mitochondria (IAN-MIT) can enter various cell types without any manipulation and improve impaired mitochondrial function in SZ-derived cells. We also show that IAN-MIT transfer enhances the previously observed impaired differentiation of SZ-derived induced pluripotent stem cells (iPSCs) into neurons.[23–25]

For in vivo effects of IAN-MIT transfer, we studied a well-established neurodevelopmental animal model of SZ, maternal immune activation, which recapitulates the well-documented association between maternal infection in pregnancy and increased risk of SZ.[26–28] In the model, injection of pregnant rats with viral mimic polyriboinosinic-polyribocytidylic acid (poly-I:C), produces in offspring a wide range of SZ-relevant, behavioral, neuroanatomical, metabolic, and immune abnormalities, including mitochondrial dysfunction.[29–35] Importantly, this model exhibits maturational delay characteristic of SZ whereby behavioral abnormalities emerge postpubertally.[29–34] Here, we show that intra-prefrontal cortex (PFC) injection of IAN-MIT to adolescent rats prenatally exposed to poly-I:C, prevents impairment in mitochondrial function in PFC neurons and emergence of SZ-like selective attention deficit in adulthood.

Materials and Methods

IAN-MIT Isolation and Transfer

IAN-MIT were isolated from Epstein–Barr virus transformed lymphocytes (lymphoblasts), derived from 3 healthy subjects (for criteria details see Rosenfeld et al[10]) or from whole brains (except the cerebellum) of 10 rats on a Percoll gradient and their purity, integrity, and activity were analyzed as previously described.[36,37] The final IAN-MIT preparation was incubated with 1 mM dehydroascorbic acid (DHA) for 5 min at 37°C before transfer. Optimal concentration for each cell type was established by validation of IAN-MIT transfer, improvement of oxygen consumption, and cell survival. IAN-MIT were stained with 5,50,6,60-tetra-chloro-1,10,3,30-tetraethyl-benzimidazolocarbocy-anine iodide (JC-1)[38] and added ($10–50$ μg protein/10^6 cells) to lymphoblasts and iPSCs. Transfer into cells was followed by Zeiss time-lapse and LSM510 Meta laser scanning confocal systems immediately and up to 24 h after transfer. As a negative control, JC-1 stained IAN-MIT were placed on the upper chamber of 0.2 μm filter trans-well, preventing mitochondria from passing through. In addition, IAN-MIT transfer into lymphoblasts was followed using common mtDNA

haplotypes, 7025(C/T) polymorphic site. Donor cells had T-base, enabling restriction with Alu1 enzyme, while host cells had C-base at this site. Three days after IAN-MIT transfer DNA was extracted (DNeasy kit Qiagene, Germany). PCR amplification of 242 bp mtDNA fragment containing the 7025(C/T) polymorphic site and an additional AGCT Alu1 site was performed (F-6890—5′-AAGCAATATGAAARGATCTG-3′; R-7131—5′-CGTAGGTTTGGTCTAGG-3′). PCR product was sequenced and separated on agarose gel, extracted, and digested by Alu1.

IAN-MIT (1.0 μg protein/10^6 cells) were also transferred into differentiating SZ-iPSCs derived from 2 controls and 2 patients on day 8 or 15 (early or late protocols, respectively) of the 6 weeks differentiation period into glutamatergic neurons. Differentiation period of late protocol was extended up to 60 days (supplementary figure S1). For functional assessments nonstained IAN-MIT were transferred.

Mitochondrial Functions

Oxygen consumption by cells was measured polarographically by Clark oxygen electrode (Strathkelvin 782 Oxygen System, Scotland) with or without dopamine (10^{-4} M).[36]

Mitochondrial $\Delta\psi_m$, cellular distribution and network connectivity in JC-1 stained cells were assessed by confocal microscopy.[10,38] In brief, $\Delta\psi_m$ was evaluated by red to green ratios, as JC-1 color alters reversibly from green (cytosol) to red (mitochondria) with increasing $\Delta\psi_m$. Uniformity of mitochondrial distribution in cells was determined by the coefficient of variation between 9 identical grid squares applied to cells. Network connectivity was determined by the extent of spreading of $\Delta\psi_m$ dissipation inside a 25× larger circle around the ROI to which a focused uncoupling laser beam was applied.

Reprogramming and Neuronal Differentiation

iPSCs reprogramming and differentiation into glutamatergic neurons through embryonic bodies were performed as previously described[25,39] (supplementary figure S1). iPSCs were reprogrammed from hair-follicle keratinocytes of 2 healthy subjects and 2 patients suffering from paranoid SZ under clozapine medication, as described previously[25] in accordance with the Ethical Committee of Rambam Medical Center. One iPSCs clone (passage 15–20) from each of the patient and control subjects was studied in 2 independent differentiation experiments in duplicates. Each iPSCs dish was divided into 2 dishes, one treated with IAN-MIT and the other with vehicle.

Immunostaining

Immunostaining of neuronal and apoptosis markers was performed and assessed as previously described.[25] Images

were captured using fluorescence microscopy (Nikon, Tokyo, Japan) connected through a video camera to a Pentium MMX-PC. Immunofluorescence-integrated density and puncta co-localization were analyzed by ImagePro (Miami, FL) and Image-J softwares (NIH, Bethesda, MD).

High-Pressure Liquid Chromatography

Concentration of consumed glutamate (Glu) and released glutamine (Gln) during 24h of culturing was assessed by high-pressure liquid chromatography (HPLC) with a fluorescence detector and analyzed as described previously.[25]

Maternal Immune Activation Model

All experimental protocols conformed the guidelines of the Institutional Animal Care and Use Committee of Tel-Aviv University and NIH. Prenatal treatment was performed as described previously.[31] On gestational day 15, pregnant Wistar dams were injected into the tail vein with poly-I:C (4 mg/kg/ml) or saline under 3% isoflurane anesthesia. On postnatal day (PND) 21, offspring were weaned and housed 2–4/cage, and a week later assigned to experimental groups. Each group consisted of male and female offspring derived from multiple independent litters.

Intracerebral IAN-MIT Injection in Adolescence

Poly-I:C and saline offspring were anesthetized with Ketamine/Xylazine cocktail (100/20 mg/kg), injected with analgesic (Rimadyl 5 mg/kg) and fixed in a stereotaxic frame (David Kopf, Germany). Freshly prepared IAN-MIT (100 μg/4.5 μl) or vehicle were injected bilaterally into the mPFC, defined as containing; cingulate gyrus 1 (AP + 2.3, ML ± 0.7, DV − 2.5), prelimbic cortex (AP + 2.3, ML ± 0.7, DV − 3.5), and infralimbic cortex (AP + 2.3, ML ± 0.7, DV − 4.9) in mm from bregma. Each rat received one bilateral injection, whereby each of these areas was injected stepwise with 33.33 μg/1.5 μl/3 min starting from the infralimbic cortex. Injections were given between PNDs 34–46, an asymptomatic period in which atypical antipsychotic drugs were shown to prevent emergence of brain and behavioral abnormalities in adult poly-I:C offspring.[30]

Latent Inhibition in Adulthood

The effects of IAN-MIT injections on selective attention were evaluated in adulthood (from PND 95) using latent inhibition (LI) test. LI reflects normal attentional capacity to ignore past-experienced stimuli as irrelevant and is disrupted in acutely psychotic SZ patients and in humans and rodents given the psychosis-inducing drug, amphetamine.[40] Prenatal poly-I:C exposure produces disrupted LI in adulthood.[30] LI was conducted as described

previously.[41] Briefly, rats were trained to drink in experimental chambers underwent 4 stages given 24 h apart: *Pre-exposure*: Bottle was removed, pre-exposed (PE) rats received 40 tones (10 s, 80 dB, 2.8 kHz) 40 s apart, whereas nonpre-exposed (NPE) rats were confined to the chamber. *Conditioning*: All rats received 2 tone-shock (0.5 mA, 1 s) pairings given 5 min apart. *Lick retraining and test*: Rats were placed in chambers with an access to the bottle. When the rat completed 75 licks, the tone was presented. Time to complete 25 licks before and after tone onset was recorded. LI is defined as a shorter time to complete licks 76–100 after tone onset (weaker fear conditioning) of the PE compared to NPE rats.

Primary Cortical Cell Line Isolation

Frontal cortex neurons from adult rats, prepared as previously described,[42] were cultured for 24 h on poly-D-lysine coated imaging glass plates before JC-1 staining.

Data Analysis

One-way ANOVA followed by Bonferroni post hoc test, 2-way ANOVA or general linear model (GLM) for repeated measurements were used. For LI, a 3-way ANOVA followed by LSD post hoc test was used. Time to complete licks 76–100 was logarithmically transformed.

Results

IAN-MIT Transfer into Various Cell Types

Fluorescence, time-lapse, and confocal microscopy confirm the nonselective ability of JC-1 labeled IAN-MIT to enter various cell types, control and SZ-derived lymphoblasts, iPSCs and H9c2 myoblasts, and stay active (figures 1A–D and supplementary figure S2). Late IAN-MIT (1.0 μg protein/10^6 cells) transfer into SZ-iPSCs led to improvement in mitochondria number and distribution in IAN-MIT treated compared to nontreated SZ-neurons at the end of the differentiation period (figure 1D). Host mitochondria remained unstained after 3 h, when their contact with JC-1 stained IAN-MIT was prevented (figure 1A-d).

IAN-MIT with mtDNA 7025 AGC/T SNP, which turns this sequence into an Alu1 restriction site, were transferred into host lymphoblasts with 7025 AGC/C mtDNA sequence (supplementary figure S2-III). Three days later following amplification and Alu1 restriction, we visualized 4 bands (167, 137, 75, and 30 bp) in IAN-MIT treated cells, while 2 bands (167 and 75 bp) in untreated cells (figure 1E). Sanger sequencing revealed a mix of 7025 C/T in IAN-MIT cells that was more pronounced upon increasing the amount of transferred IAN-MIT (supplementary figure S2-III). Thus, both host and donor mtDNA are present in IAN-MIT treated cells for at least 3 days after transfer.
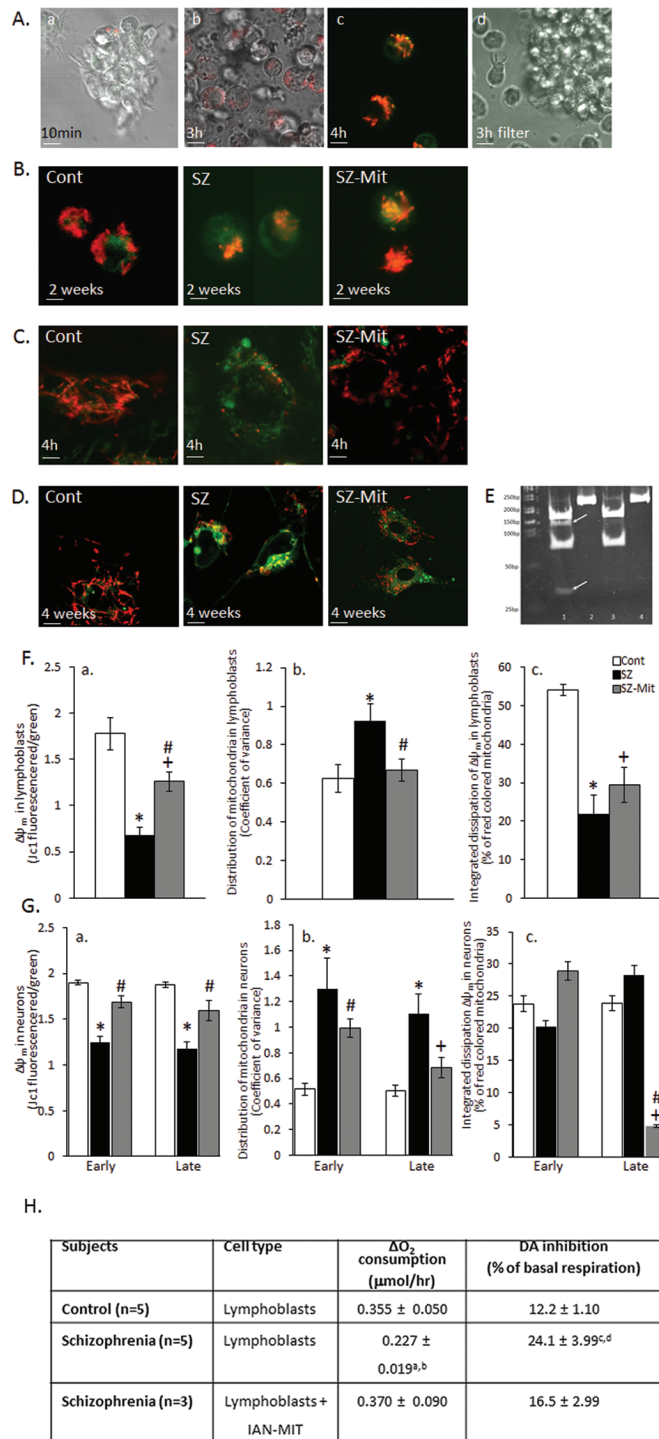
Fig. 1. Mitochondrial transfer into healthy and SZ cells. **(A)** Representative images of time-dependent transfer of JC-1 stained IAN-MIT into SZ-lymphoblasts, **(a**, **b)** by time-lapse, **(c)** confocal microscopy, and **(d)** JC-1 stained IAN-MIT negative control. **(B–D)** Representative images of JC-1 stained cells **(B)** 2 weeks after transfer into lymphoblasts, **(C)** 4 h after transfer into iPSCs, **(D)** 4 weeks after late IAN-MIT transfer in neurons. **(E)** PCR products 3 days after IAN-MIT (4 bands) or vehicle (2 bands) with (lanes 1 and 3) and without Alu1 restriction (lanes 2 and 4). **(F)** Quantification in lymphoblasts of **(a)** $\Delta\psi_m$, **(b)** mitochondrial distribution, **(c)** network connectivity. IAN-MIT normalized $\Delta\psi_m$ and mitochondria distribution impairments, but not network connectivity. **(G)** Quantification in neurons of **(a)** $\Delta\psi_m$, **(b)** mitochondrial distribution, and **(c)** network connectivity. IAN-MIT normalized the impaired $\Delta\psi_m$ and mitochondria cellular distribution observed in SZ-neurons. JC-1 in cytosol (green) and in active mitochondria (red). Values are mean ± SEM of 2 controls and 2 patients (one iPSCs clone for each) from 2 experiments in duplicates with 5–6 cells in each. Scale bars: A—1 μm (time-lapse) and 3 μm (confocal), B and C—5 μm, D—2 μm. *$P < .02$, SZ vs Cont; +$P < .01$, SZ-Mit vs Cont; #$P < .03$, SZ-Mit vs SZ. **(H)** IAN-MIT transfer restores abnormal respiration rates and dopamine-induced inhibition in SZ-lymphoblasts 25 days (5 passages) after transfer. [a]$P < .04$ and [c]$P < .004$ vs control; [b]$P < .03$ and [d]$P < .025$ vs lymphoblasts + Mit.

Approximately 50% of the lymphoblasts took-up stained IAN-MIT following treatment with 50 μg IAN-MIT protein/10^6 cells and 3 days later 15%–20% of mtDNA originated from IAN-MIT was still present.

IAN-MIT Transfer and Mitochondrial Function

IAN-MIT transfer normalized the impaired basal respiration observed in SZ-lymphoblasts. Furthermore, dopamine inhibitory effect on respiration, which is two-fold higher in SZ than in healthy cells,[36,43,44] was normalized by IAN-MIT transfer (figure 1H). This protective effect of IAN-MIT lasted up to 25 days and then gradually declined. Following IAN-MIT transfer $\Delta\psi_m$ dissipation observed in SZ-cells was improved ($P < .026$, SZ-Mit vs SZ) (figure 1F-a) and a uniform mitochondrial distribution, compared to the aggregated pattern in SZ-lymphoblasts, was detected ($P < .025$, SZ-Mit vs SZ) (figure 1F-b). However, IAN-MIT transfer had no beneficial effect on mitochondrial network connectivity (figure 1F-c).

In neurons, both early and late IAN-MIT transfer into differentiating iPSCs recovered $\Delta\psi_m$ ($P < .001$, $P < .012$, SZ-Mit vs SZ, respectively) (figure 1G-a). However, only after late transfer, the uneven distribution of mitochondria observed in SZ-neurons, was normalized ($P < .03$, SZ-Mit vs SZ) and not significantly different from controls (figure 1G-b). We previously reported that mitochondrial network connectivity in SZ-iPSCs derived glutamatergic neurons was similar to that of controls. In contrast, following late, but not early IAN-MIT transfer, a reduction in connectivity was observed compared to both control ($P < .017$) and SZ ($P < .004$), suggesting low connectivity between host and transferred mitochondria (figure 1G-c). Supplementary table S1 presents individual data.

IAN-MIT Transfer and iPSCs Differentiation

Both early and late IAN-MIT transfer into SZ-cells improved neuronal differentiation compared to untreated SZ-cells (figure 2 and supplementary table S2). However, differentiation efficiency, expressed by specific markers, was significantly enhanced by late as compared to early transfer. Thus, early transfer resulted in increased expression ($P < .04$) of β3-tubulin (neuronal marker) but not of Tbr1 (glutamatergic maturation marker), while following late transfer both markers (β3-tubulin—$P < .029$; Tbr1—$P < .001$) were increased in SZ-Mit-neurons as compared to SZ-neurons (figures 2B and 2D), with no significant difference from controls in β3-tubulin. Tbr1 expression did not reach control levels even following extended differentiation period, yet GLM analysis showed a time-dependent increase in Tbr1 ($P < .001$) and in β3-tubulin ($P < .002$) in SZ-Mit-neurons. Early transfer did not cause any improvement in PSD-95 or synapsin1, post- and presynaptic markers, respectively, while late transfer ameliorated synapsin1 ($P < .016$), but not PSD-95 in SZ-Mit-neurons as compared to SZ-neurons (figures 2C and 2E). GLM analysis showed a time-dependent increase in synapsin1 during differentiation ($P < .002$), which following extended differentiation was not significantly different from controls. Both early and late IAN-MIT transfer did not improve co-localization of synapsin1 and PSD-95, an accepted indicator of synaptic contacts, yet extending differentiation period increased co-localization ($P < .017$) in SZ-Mit as compared to SZ-neurons. At the end of the extended protocol, neurons number decreased, yet both differentiation and maturation markers were enhanced in SZ-Mit surviving neurons.

In SZ, neural glutamate delivery via the glutamate-glutamine (Glu-Gln) cycle, a fundamental interaction between astrocytes and glutamatergic neurons, is disrupted.[45,46] HPLC analysis showed that late, but not early, transfer of IAN-MIT increased Glu consumption expressed by its lower levels in SZ-Mit culture medium as compared to SZ-neurons ($P < .05$). Concomitantly, higher levels of released Gln were observed in SZ-Mit-neurons ($P < .014$ vs SZ), reaching control levels (figures 2F and 2G and supplementary table S3), suggesting an almost normalized activation of the Glu-Gln cycle following late IAN-MIT transfer.

IAN-MIT Transfer and Apoptosis

An additional function of mitochondria is their involvement in apoptosis. In SZ-iPSCs and their differentiated neurons spontaneous and H_2O_2-induced apoptosis, assessed by Bcl-2/Bax ratio and DNA fragmentation, was significantly impaired. Transfer of IAN-MIT had no significant effect on spontaneous or H_2O_2-induced parameters (supplementary data and supplementary figure S3).

IAN-MIT transfer into control subjects-derived cells had no effect on any of the studied parameters (figure 3).

LI in Poly-I:C Rats

The experiment included 8 experimental groups (n/group=7–9, overall $n = 67$) in a $2 \times 2 \times 2$ factorial design with main factors of pre-exposure (NPE, PE), prenatal treatment (saline, poly-I:C), and intracortical injection (IAN-MIT, vehicle). The groups did not differ in times to complete licks 51–75 prior to tone onset ($P > .05$). LI, namely, lower suppression of drinking of the PE compared to NPE rats, was present in vehicle injected offspring of saline dams but not of poly-I:C. IAN-MIT injection restored LI in poly-I:C rats but disrupted LI in controls (figure 4A). Three-way ANOVA yielded main effects of pre-exposure [$F(1, 66) = 14.96$; $P < .001$], interactions of prenatal treatment × intracortical injection [$F(1, 66) = 12.22$; $P < .001$] and pre-exposure ×
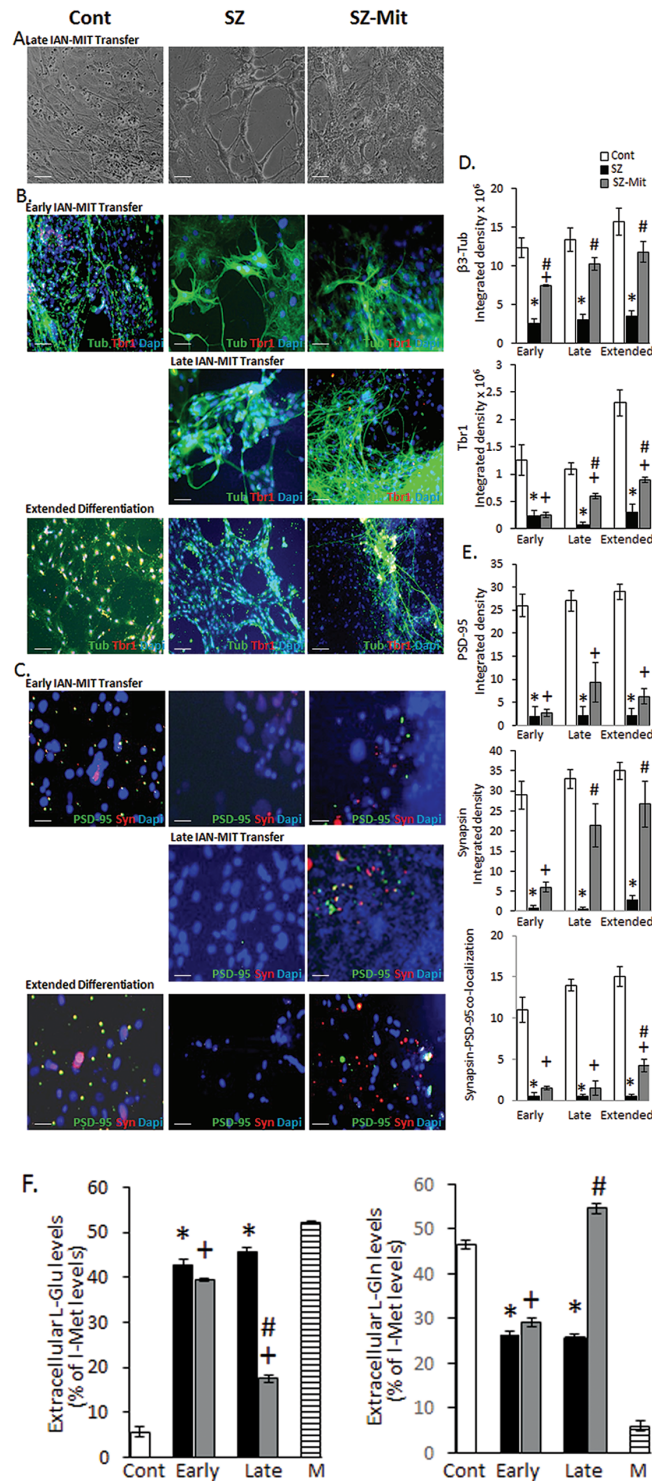
Fig. 2. Glutamatergic differentiation following early and late IAN-MIT transfer. (**A**) Bright-field images of neurons. (**B**) Immunofluorescence staining and (**D**) quantification of β3-tubulin and Tbr1, both decreased in SZ neurons. Early and late IAN-MIT transfer increased β3-tubulin, while Tbr1 increased only following late transfer. GLM analysis showed a time-dependent increase in both (β3-tubulin–F = 20.16, P < .001. Tbr1-F = 116.8, P < .001). (**C**) Immunofluorescence staining and (**E**) quantification of synapsin1 and PSD-95 and their co-localization, which were decreased in SZ-neurons. Early and Late IAN-MIT transfer had a minor effect on PSD-95 and co-localization, yet profoundly affected synapsin1, which following late transfer reached control levels. GLM showed a time-dependent increase in synapsin1 (Synapsin1-F = 90.15, P < .002). Values are mean ± SEM of 2 controls and 2 patients (one iPSCs clone for each) from 2 experiments in duplicates with 4–6 cells in each. Scale bars: A, B—100 μm, C—25 μm. (**F**) Late, but not early, IAN-MIT transfer almost normalized Gln release and ameliorated abnormal Glu consumption. Values are mean ± SEM of 2 controls and 2 patients (one iPSCs clone for each) from 2 experiments in triplicates. *P < .01 SZ vs Cont; +P < .008 SZ-Mit vs Cont; #P < .03 SZ-Mit vs SZ.
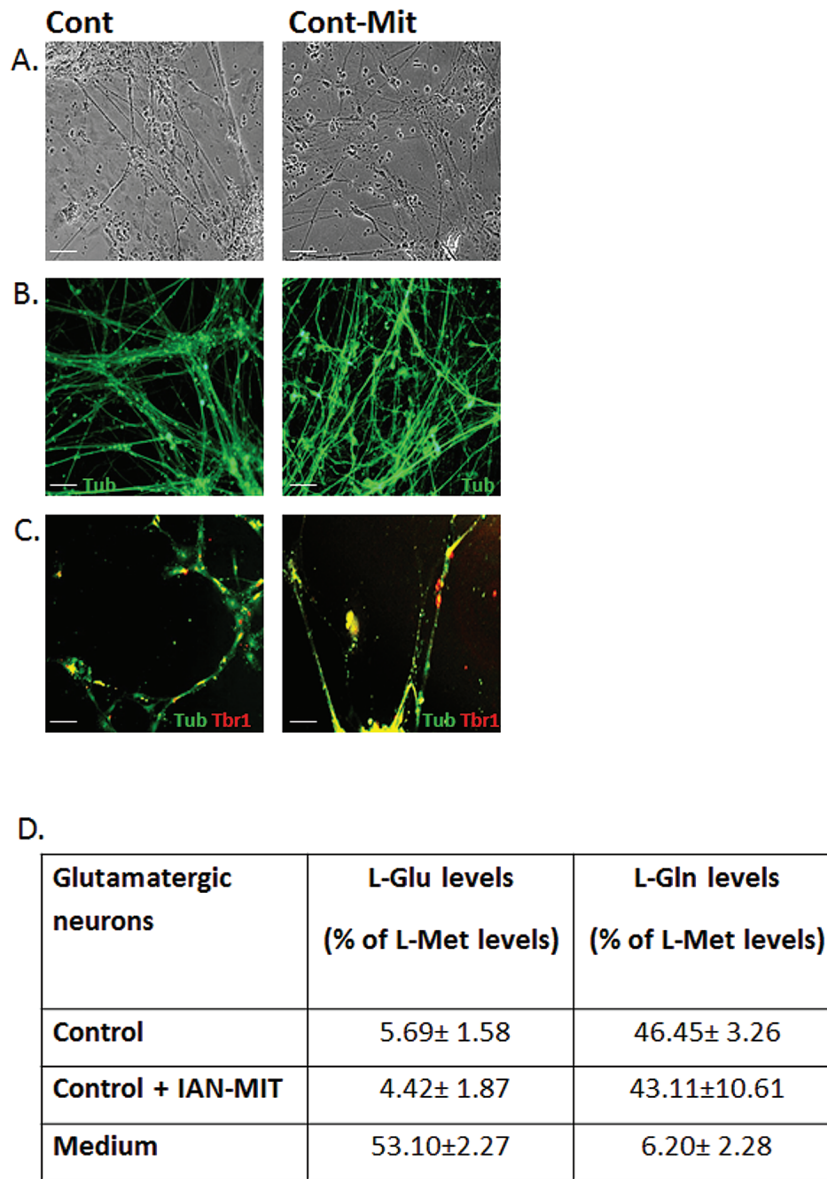
Fig. 3. IAN-MIT late transfer had no effect on differentiation of control-derived iPSC. (A) Bright field images of neurons. (B) Immunofluorescence staining of β3-tubulin and (C) Tbr1. Scale bar:100 μm. (D) Glu consumption and Gln release in control neurons. Values are mean ± SEM of 2 controls (one iPSCs clone for each) from 2 experiments in duplicates.

prenatal treatment × intracortical injection [$F_{(1, 66)}$ = 8.02; $P < .05$]. Post hoc comparisons confirmed the presence of LI in poly-I:C-IAN-MIT, and saline-vehicle conditions ($P < .005$) but not in the poly-I:C-vehicle, and saline-IAM-MIT condition.

IAN-MIT and $\Delta\psi_m$ in Frontal Cortex Neurons

A significant reduction (26%) in mitochondrial $\Delta\psi_m$ was observed in poly-I:C compared to saline exposed offspring [$F_{(1, 18)}$ = 6.697; $P < .05$]. IAN-MIT injection increased mitochondrial $\Delta\psi_m$ in both poly-I:C and saline exposed offspring compared to vehicle injected animals [$F_{(1, 18)}$ = 4.748; $P < .05$)]. IAN-MIT had no effect on mitochondrial distribution and network connectivity (figures 4B and 4C).

Discussion

This study demonstrates the ability of heterologous IAN-MIT to enter, without manipulation, different cell types and induce long-lasting improvement in mitochondrial functions and in the differentiation of SZ-iPSCs into neurons. Furthermore, in the poly-I:C rat model, intra-mPFC IAN-MIT injection prevented dissipation in $\Delta\psi_m$, a vital component of active mitochondria and the driving force of ATP production, as well as attentional deficit.

The ability of IAN-MIT to enter various cell types within a few minutes, suggests that it is a general cellular competence. IAN-MIT entrance and short-term survival were followed by staining them with JC-1 and the presence of their mtDNA haplotype in host cells for at
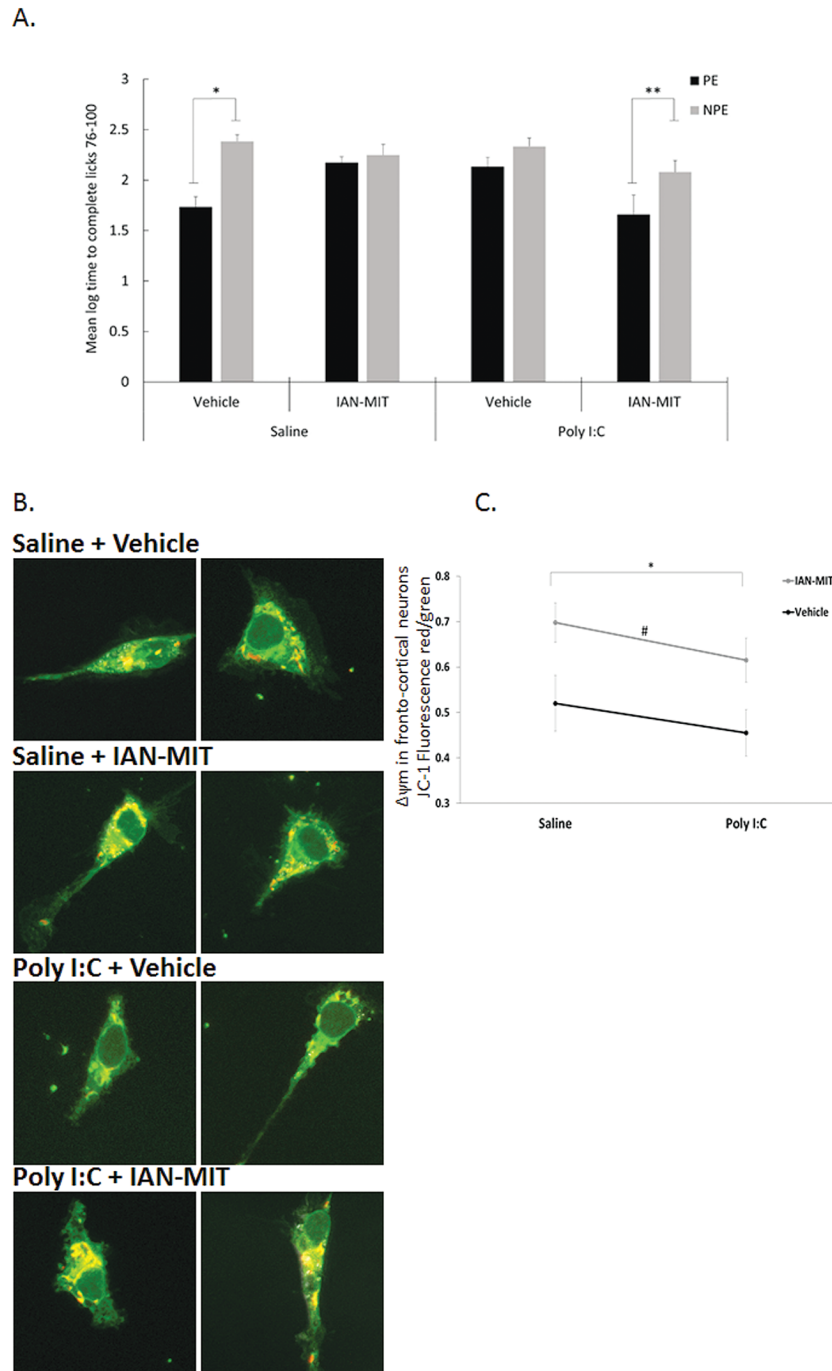
Fig. 4. mPFC IAN-MIT transfer prevents disrupted LI and dissipated $\Delta\psi_m$ in poly-I:C exposed offspring. (**A**) LI is manifested as shorter log times to complete licking criteria after tone onset of PE compared with NPE groups. Values are mean ± SEM. *P < .0001 PE vs NPE in saline-vehicle exposed offspring and in poly-I:C+IAN-MIT exposed offspring. (**B**) Representative images of JC-1 stained cortical neurons. JC-1 in cytosol (green), in active mitochondria (red). Scale bar: 5 μm. (**C**) Quantification of $\Delta\psi_m$, which is reduced in poly-I:C rats and increased by IAN-MIT injection in both poly-I:C and saline exposed offspring (n = 4–5 rats/group) *P < .04 IAN-MIT vs Vehicle. #P < .02 Poly-I:C vs Saline.

least 3 days. Long-term effects were demonstrated by mitochondrial functional improvement in SZ-derived lymphoblasts and iPSCs improved differentiation several weeks after treatment. The long-lasting beneficial effect of IAN-MIT on respiration suggests either that donor mitochondria survive or their mtDNA is transferred into host mitochondria. However, the long-lasting normalization of dopamine-induced inhibition of respiration,

suggests that donor mitochondria survived for at least a few weeks, since dopamine interacts with complex-I at a site comprised of nuclear encoded subunits.[36]

The mechanism by which mitochondria transfer from the extracellular matrix into cells is still unknown and is probably different from their transfer between cells through junctions, cell fusion, and tunneling nanotube formation.[17,20] It is well-documented that cell-to-cell communication involves release and uptake of extracellular particles of mitochondrial size (0.5–1 μm) by macropinocytosis, a form of endocytosis that accompanies cell surface ruffling.[47,48] Recently, it was reported that astrocytes' released mitochondria can enter adjacent neurons and enhance neuronal survival and plasticity after ischemia.[22] Actin-dependent endocytosis was suggested for extracellular autologous mitochondria uptake by cardiomyocytes.[19,49]

We and others have previously shown impaired ability of SZ-iPSCs to differentiate into glutamatergic neurons.[23,25,50] Here, we demonstrate a direct link between mitochondrial function and differentiation efficiency of these neurons, assessed by increased expression of matured glutamatergic neurons markers, number of synaptic contacts, and normalization of the Glu-Gln cycle. Glutamine synthase in healthy brains is restricted to astrocytes, but our differentiating iPSCs probably contain additional cell types, which may mimic astrocyte function and convert Glu to Gln. Moreover, in cell culture and in diseased brains, as in Alzheimer's disease, glutamine synthase has been observed in neurons.[46]

Timing of IAN-MIT transfer during differentiation was critical, as SZ-neurons differentiation was significantly enhanced following late compared to early transfer. This timing-dependent difference may be due to a reduction in cell division rate along differentiation that impacts host newly synthesized mitochondria. This is supported by reduced network connectivity in SZ-Mit neurons following late, yet not early transfer, suggesting that more IAN-MIT, failing to fuse with host mitochondria, remain. In this regard, it is worth mentioning that in dividing SZ-lymphoblasts, beneficial effect of IAN-MIT transfer on cell respiration gradually declined after a few weeks. The importance of timing may be also linked to the gradual transformation from mainly glycolysis early in differentiation, into the more efficient OXPHOS source of energy later in differentiation,[51] when a need for active healthy mitochondria becomes more critical.

The improvement in differentiation by IAN-MIT is only partial, suggesting the need for additional factors to enhance differentiation. Still, in neurodevelopmental disorders such as SZ, a partial amelioration, due to treatment at specific time-windows and brain areas, may suffice to improve brain and behavioral abnormalities. In support of the latter, we found that IAN-MIT injection into the mPFC of adolescent poly-I:C rats, a period during which the brain undergoes a second phase of growth,[52] exerted long-term effects on mitochondrial function and attentional capacity. Specifically, we show that $\Delta\psi_m$ in PFC neurons of adult poly-I:C offspring is dissipated, consistent with previous findings of reduced mitochondrial ATP production in splenocytes,[53] increased brain mitochondrial respiratory chain activity, and decreased oxygen consumption in such rats.[35] However, injection of IAN-MIT at adolescence prevented $\Delta\psi_m$ deficit. Furthermore, we show that this intervention prevents selective attention deficit that normally emerges in adult poly-I:C offspring. To the best of our knowledge, this is the first demonstration that transfer of healthy mitochondria has long-term beneficial effect on mitochondrial function and can rescue cognitive function, at a long delay from the intervention. The mechanisms underlying these effects remain to be elucidated. Long-term deleterious effects of prenatal poly-I:C exposure are believed to be mediated by developmental neuroinflammation.[54] Given the mounting evidence linking mitochondrial dysfunction and inflammation,[55–59] it is possible that improvement of mitochondrial function reduces neuroinflammation.

In control rats, IAN-MIT increased mitochondrial membrane potential and disrupted LI. This may suggest that in vivo IAN-MIT transfer is beneficial when mitochondrial function is impaired, while under normal conditions it interferes with mitochondrial function homeostasis. While the relationship between mitochondrial and attentional functions is not known, the pattern obtained in controls and poly-I:C offspring, namely, improvement of both mitochondrial and attentional functions in poly-I:C offspring and disruption of both in controls, provides some support for such a relationship.

Mitochondria are multi-edged swords involved in various cellular processes, either supporting cell survival or leading to cell death. This toxicity may limit the use of IAN-MIT transfer. However, this tendency of mitochondria is at least in part dependent on their activity state. In this study, toxicity was restrained by treating mitochondria with the antioxidant DHA[60] and by assuring that isolated mitochondria are normally active, producing fewer free electrons and consequently fewer superoxide products.[61] Consistent with the latter is IAN-MIT lack of effects on control cells and on the impaired apoptosis observed in SZ cells. However, their deleterious effect in vivo in control rats calls for a careful optimization of dose and conditions.

In this study, we used heterologous mitochondria, since autologous mitochondria is not applicable in SZ, where mitochondrial deficits are observed in peripheral cells. Heterologous mitochondria may induce an inflammatory response, as cellular injury can release mitochondrial DNA and proteins that can activate innate immunity.[62] Although, several studies showed that transfer of mitochondria does not induce inflammation or autoimmune response,[19,21] this needs to be investigated in future studies.

Taken together, the present findings suggest a beneficial effect of IAN-MIT transfer both in vitro and in vivo. Only a few cell lines and processes were studied, therefore further experiments are warranted to address various issues such as SZ heterogeneity, inter- and intravariation between hiPSCs, mitochondria transfer-induced inflammation and the mechanisms by which IAN-MIT induce their effects in vitro and in vivo. Still, in the context of SZ, the findings suggest that mitochondria can enter cells, improve their mitochondrial activity, support neuronal differentiation and restore functional deficits.

Supplementary Material

Supplementary data are available at *Schizophrenia Bulletin* online.

References

1. Cho B, Choi SY, Cho HM, Kim HJ, Sun W. Physiological and pathological significance of dynamin-related protein 1 (drp1)-dependent mitochondrial fission in the nervous system. *Exp Neurobiol*. 2013;22:149–157.

2. Ben-Shachar D, Laifenfeld D. Mitochondria, synaptic plasticity, and schizophrenia. *Int Rev Neurobiol*. 2004;59:273–296.

3. Sun T, Qiao H, Pan PY, Chen Y, Sheng ZH. Motile axonal mitochondria contribute to the variability of presynaptic strength. *Cell Rep*. 2013;4:413–419.

4. Díaz-Castro B, Pardal R, García-Flores P, et al. Resistance of glia-like central and peripheral neural stem cells to genetically induced mitochondrial dysfunction—differential effects on neurogenesis. *EMBO Rep*. 2015;16:1511–1519.

5. Rangaraju V, Calloway N, Ryan Timothy A. Activity-driven local ATP synthesis is required for synaptic function. *Cell*. 2014;156:825–835.

6. Sun T, Qiao H, Pan PY, Chen Y, Sheng ZH. Motile axonal mitochondria contribute to the variability of presynaptic strength. *Cell Rep*. 2013;4:413–419.

7. Ben-Shachar D. Mitochondrial multifaceted dysfunction in schizophrenia; complex I as a possible pathological target. *Schizophr Res*. 2016. pii: S0920-9964(16)30466-2.

8. Manji H, Kato T, Di Prospero NA, et al. Impaired mitochondrial function in psychiatric disorders. *Nat Rev Neurosci*. 2012;13:293–307.

9. Sequeira A, Martin MV, Rollins B, et al. Mitochondrial mutations and polymorphisms in psychiatric disorders. *Front Genet*. 2012;3:103.

10. Rosenfeld M, Brenner-Lavie H, Ari SG, Kavushansky A, Ben-Shachar D. Perturbation in mitochondrial network dynamics and in complex I dependent cellular respiration in schizophrenia. *Biol Psychiatry*. 2011;69:980–988.

11. Iwamoto K, Bundo M, Kato T. Altered expression of mitochondria-related genes in postmortem brains of patients with bipolar disorder or schizophrenia, as revealed by large-scale DNA microarray analysis. *Hum Mol Genet*. 2005;14:241–253.

12. Prabakaran S, Swatton JE, Ryan MM, et al. Mitochondrial dysfunction in schizophrenia: evidence for compromised brain metabolism and oxidative stress. *Mol Psychiatry*. 2004;9:684–687, 643.

13. Dror N, Klein E, Karry R, et al. State-dependent alterations in mitochondrial complex I activity in platelets: a potential peripheral marker for schizophrenia. *Mol Psychiatry*. 2002;7:995–1001.

14. Maurer I, Zierz S, Möller H. Evidence for a mitochondrial oxidative phosphorylation defect in brains from patients with schizophrenia. *Schizophr Res*. 2001;48:125–136.

15. Bergman O, Ben-Shachar D. Mitochondrial oxidative phosphorylation system (OXPHOS) deficits in schizophrenia: possible interactions with cellular processes. *Can J Psychiatry*. 2016;61:457–469.

16. Gerdes HH, Bukoreshtliev NV, Barroso JF. Tunneling nanotubes: a new route for the exchange of components between animal cells. *FEBS Lett*. 2007;581:2194–2201.

17. Islam MN, Das SR, Emin MT, et al. Mitochondrial transfer from bone-marrow-derived stromal cells to pulmonary alveoli protects against acute lung injury. *Nat Med*. 2012;18:759–765.

18. Tan An S, Baty James W, Dong L-F, et al. Mitochondrial genome acquisition restores respiratory function and tumorigenic potential of cancer cells without mitochondrial DNA. *Cell Metabolism*. 2015;21:81–94.

19. Masuzawa A, Black KM, Pacak CA, et al. Transplantation of autologously derived mitochondria protects the heart from ischemia-reperfusion injury. *Am J Physiol Heart Circ Physiol*. 2013;304:H966–H982.

20. Spees JL, Olson SD, Whitney MJ, Prockop DJ. Mitochondrial transfer between cells can rescue aerobic respiration. *Proc Natl Acad Sci U S A*. 2006;103:1283–1288.

21. McCully JD, Levitsky S, Del Nido PJ, Cowan DB. Mitochondrial transplantation for therapeutic use. *Clin Transl Med*. 2016;5:16.

22. Hayakawa K, Esposito E, Wang X, et al. Transfer of mitochondria from astrocytes to neurons after stroke. *Nature*. 2016;535:551–555.

23. Brennand KJ, Simone A, Jou J, et al. Modelling schizophrenia using human induced pluripotent stem cells. *Nature*. 2011;473:221–225.

24. Pedrosa E, Sandler V, Shah A, et al. Development of patient-specific neurons in schizophrenia using induced pluripotent stem cells. *J Neurogenet*. 2011;25:88–103.

25. Robicsek O, Karry R, Petit I, et al. Abnormal neuronal differentiation and mitochondrial dysfunction in hair follicle-derived induced pluripotent stem cells of schizophrenia patients. *Mol Psychiatry*. 2013;18:1067–1076.

26. Adams W, Kendell RE, Hare EH, Munk-Jørgensen P. Epidemiological evidence that maternal influenza contributes to the aetiology of schizophrenia. An analysis of Scottish, English, and Danish data. *Br J Psychiatry*. 1993;163:522–534.

27. O'Callaghan E, Sham PC, Takei N, et al. The relationship of schizophrenic births to 16 infectious diseases. *Br J Psychiatry*. 1994;165:353–356.

28. Torrey EF, Rawlings R, Waldman IN. Schizophrenic births and viral diseases in two states. *Schizophr Res*. 1988;1:73–77.

29. Piontkewitz Y, Arad M, Weiner I. Abnormal trajectories of neurodevelopment and behavior following in utero insult in the rat. *Biol Psychiatry*. 2011;70:842–851.

30. Piontkewitz Y, Arad M, Weiner I. Tracing the development of psychosis and its prevention: what can be learned from animal models. *Neuropharmacology*. 2012;62:1273–1289.

31. Zuckerman L, Rehavi M, Nachman R, Weiner I. Immune activation during pregnancy in rats leads to a postpubertal emergence of disrupted latent inhibition, dopaminergic hyperfunction, and altered limbic morphology in the offspring: a novel neurodevelopmental model of schizophrenia. *Neuropsychopharmacology*. 2003;28:1778–1789.

32. Meyer U, Feldon J, Schedlowski M, Yee BK. Towards an immuno-precipitated neurodevelopmental animal model of schizophrenia. *Neurosci Biobehav Rev*. 2005;29:913–947.

33. Giovanoli S, Engler H, Engler A, et al. Stress in puberty unmasks latent neuropathological consequences of prenatal immune activation in mice. *Science*. 2013;339:1095–1099.

34. Meyer U. Prenatal poly(i:C) exposure and other developmental immune activation models in rodent systems. *Biol Psychiatry*. 2014;75:307–315.

35. Naviaux RK, Zolkipli Z, Wang L, et al. Antipurinergic therapy corrects the autism-like features in the poly(IC) mouse model. *PLoS One*. 2013;8:e57380.

36. Brenner-Lavie H, Klein E, Zuk R, Gazawi H, Ljubuncic P, Ben-Shachar D. Dopamine modulates mitochondrial function in viable SH-SY5Y cells possibly via its interaction with complex I: relevance to dopamine pathology in schizophrenia. *Biochim Biophys Acta*. 2008;1777:173–185.

37. Sims NR, Anderson MF. Isolation of mitochondria from rat brain using Percoll density gradient centrifugation. *Nat Protoc*. 2008;3:1228–1239.

38. Ben-Shachar D, Suss-Toby E, Robicsek O. Analysis of mitochondrial network by imaging: proof of technique in schizophrenia. *Methods Mol Biol*. 2015;1265:425–439.

39. Petit I, Kesner NS, Karry R, et al. Induced pluripotent stem cells from hair follicles as a cellular model for neurodevelopmental disorders. *Stem Cell Res*. 2012;8:134–140.

40. Weiner I. The "two-headed" latent inhibition model of schizophrenia: modeling positive and negative symptoms and their treatment. *Psychopharmacology (Berl)*. 2003;169:257–297.

41. Zuckerman L, Weiner I. Post-pubertal emergence of disrupted latent inhibition following prenatal immune activation. *Psychopharmacology (Berl)*. 2003;169:308–313.

42. Brewer GJ, Torricelli JR. Isolation and culture of adult neurons and neurospheres. *Nat Protoc*. 2007;2:1490–1498.

43. Ben-Shachar D, Zuk R, Gazawi H, Ljubuncic P. Dopamine toxicity involves mitochondrial complex I inhibition: implications to dopamine-related neuropsychiatric disorders. *Biochem Pharmacol*. 2004;67:1965–1974.

44. Brenner-Lavie H, Klein E, Ben-Shachar D. Mitochondrial complex I as a novel target for intraneuronal DA: modulation of respiration in intact cells. *Biochem Pharmacol*. 2009;78:85–95.

45. Hashimoto K, Engberg G, Shimizu E, Nordin C, Lindström LH, Iyo M. Elevated glutamine/glutamate ratio in cerebrospinal fluid of first episode and drug naive schizophrenic patients. *BMC Psychiatry*. 2005;5:6.

46. Fernandes SP, Dringen R, Lawen A, Robinson SR. Neurones express glutamine synthetase when deprived of glutamine or interaction with astrocytes. *J Neurochem*. 2010;114:1527–1536.

47. Swanson JA, Watts C. Macropinocytosis. *Trends Cell Biol*. 1995;5:424–428.

48. Mulcahy LA, Pink RC, Carter DR. Routes and mechanisms of extracellular vesicle uptake. *J Extracell Vesicles*. 2014;3. doi:10.3402/jev.v3.24641.

49. Pacak CA, Preble JM, Kondo H, et al. Actin-dependent mitochondrial internalization in cardiomyocytes: evidence for rescue of mitochondrial function. *Biol Open*. 2015;4:622–626.

50. Brennand K, Savas JN, Kim Y, et al. Phenotypic differences in hiPSC NPCs derived from patients with schizophrenia. *Mol Psychiatry*. 2015;20:361–368.

51. Panopoulos AD, Yanes O, Ruiz S, et al. The metabolome of induced pluripotent stem cells reveals metabolic changes occurring in somatic cell reprogramming. *Cell Res*. 2012;22:168–177.

52. Bandeira F, Lent R, Herculano-Houzel S. Changing numbers of neuronal and non-neuronal cells underlie postnatal brain growth in the rat. *Proc Natl Acad Sci U S A*. 2009;106:14108–14113.

53. Giulivi C, Napoli E, Schwartzer J, Careaga M, Ashwood P. Gestational exposure to a viral mimetic poly(i:C) results in long-lasting changes in mitochondrial function by leucocytes in the adult offspring. *Mediators Inflamm*. 2013;2013:609602.

54. Meyer U. Developmental neuroinflammation and schizophrenia. *Prog Neuropsychopharmacol Biol Psychiatry*. 2013;42:20–34.

55. López-Armada MJ, Riveiro-Naveira RR, Vaamonde-García C, Valcárcel-Ares MN. Mitochondrial dysfunction and the inflammatory response. *Mitochondrion*. 2013;13:106–118.

56. West AP, Shadel GS, Ghosh S. Mitochondria in innate immune responses. *Nat Rev Immunol*. 2011;11:389–402.

57. Arnoult D, Soares F, Tattoli I, Girardin SE. Mitochondria in innate immunity. *EMBO Rep*. 2011;12:901–910.

58. Cloonan SM, Choi AM. Mitochondria: commanders of innate immunity and disease? *Curr Opin Immunol*. 2012;24:32–40.

59. Krysko DV, Agostinis P, Krysko O, et al. Emerging role of damage-associated molecular patterns derived from mitochondria in inflammation. *Trends Immunol*. 2011;32:157–164.

60. Li X, Cobb CE, Hill KE, Burk RF, May JM. Mitochondrial uptake and recycling of ascorbic acid. *Arch Biochem Biophys*. 2001;387:143–153.

61. Kudin AP, Malinska D, Kunz WS. Sites of generation of reactive oxygen species in homogenates of brain tissue determined with the use of respiratory substrates and inhibitors. *Biochim Biophys Acta*. 2008;1777:689–695.

62. Zhang Q, Raoof M, Chen Y, et al. Circulating mitochondrial DAMPs cause inflammatory responses to injury. *Nature*. 2010;464:104–107.